

## 20th of July 2007 tornado - towards prediction

JAN PARFINIEWICZ

*Institute of Meteorology and Water Management 61 Podlesna str., PL-01673 Warsaw, Poland*

### 1. Introduction

A multi-scale synoptic analysis of the 8-minute tornado case in Poland has been performed based on 3D Virtual Synoptic Laboratory concept. The key issue of How to predict a similar tornado in the future? has been analyzed, taking into account the predictability potential of particular components of the system. This text, as additional to Newsletters No. 9 - 10 (Parfiniewicz, 2008,2010), will focus on predictability analysis heading for final conclusion (hoping for being useful when organizing operational short term warning system).

*About the case.* On July 20, 2007, about 16:05 UTC, the Czestochowa district was struck by tornado, which destroyed dwellings, farm buildings, transmission lines and poles, falling down tens of hectares of forest, and displacing automobiles. Strong hailstorms were observed an hour before, during, and after the tornado. According to the eyewitness reports, the hailstones were initially of pea size, then large and irregular ice pieces, some 5 cm or more in diameter. The ground was covered by a thick ice layer reaching to the knees. During the tornado and right afterwards, horizontally moving hailstones of a tennis-ball size were observed. The tornado trail was about 14 km long and the destruction track was up to 500 m wide. The mean speed of displacement was around 45 km/h. On the basis of the type of damage, the tornado was classified as between F1 and F2 in Fujita-Pearson scale or T4 in the 11-step TORRO scale. The wind speed in the vortex could reach 60 m/s (Bebot et al., 2007).

### 2. Synoptic background

To carry out analysis there was created something like Virtual Synoptic Laboratory (based on 3D visualization) using Vis5d and elaborating a number of tools like the one to produce reflectivity composites and Doppler retrievals. It was recognized that the dominant driving process for the abrupt convection over Europe was an inflow in the upper troposphere of a cold arctic air over a warm and humid tropical air. Deep massive drop of cold Arctic air started moving over the Atlantic from Greenland towards the British Isles, eventually modifying the formation of the Atlantic branch of the polar jet stream. After 8 days of the cold air movement over North Atlantic, the Atlantic branch of the jet stream extended north-easterly over Europe parallel to elongated tongue of hot and moist tropical air masses on its east side (Newsletter 9). The synoptic situation was difficult to analyze, as evidenced by differences in the MSL synoptic analysis made by English, German, Dutch, and Polish services and points to a difficulty in working out a concept of how to analyze the development of upper fronts. The NWP model outputs ran on 14 km grid size with 35 levels has been used to demonstrate the process. 3D inspection of the potential temperature topography shows quite significant slope of 315 K isentropic surface - the upper cold front. And this cross-isobaric sliding over hot subtropical air beneath must have been responsible for the abrupt convection. The W-E vertical cross-section of potential temperature, with overlapping radars reflectivity at 16

UTC (Fig. 1) demonstrates that a process of this type generates the so-called convective alias potential instability and releases a strong convection.

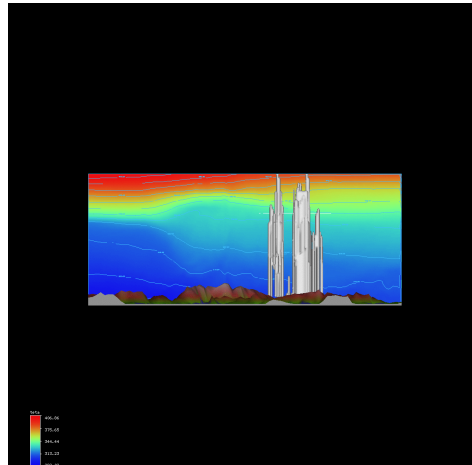


Figure 1: W-E cross section potential temperature + reflectivity at 16 UTC on 20 July 2007

The following steps in the development of the convective situation were distinguished:

- [A] Nocturnal disintegration of the preceding convective complex; 00-04 UTC,
- [B] Development and disintegration of individual convective cells; 04-10 UTC,
- [C] Formation of a convective cluster, and an initiating cell for a further supercell formation, i.e., a very strongly moving and abruptly upwelling huge cumulonimbus cloud; 10-14 UTC,
- [D] Formation of a supercell from the merging of slowly-moving clockwise convective complex with a huge cumulonimbus cloud abruptly upwelling, being embedded in the positive vorticity region; 14-16 UTC,
- [E] Mature supercell stage, with a tornado in the Czestochowa region (16:05 - 16:15 UTC) and a convective complex originated over the Tatra mountains and Slovakia; 16-18 UTC.

We will now focus on the supercell transition from early to mature stage, step [D] to [E] (Fig. 2(a)-2(b)) (for more, see Newsletter 9, Fig.9 a - f).

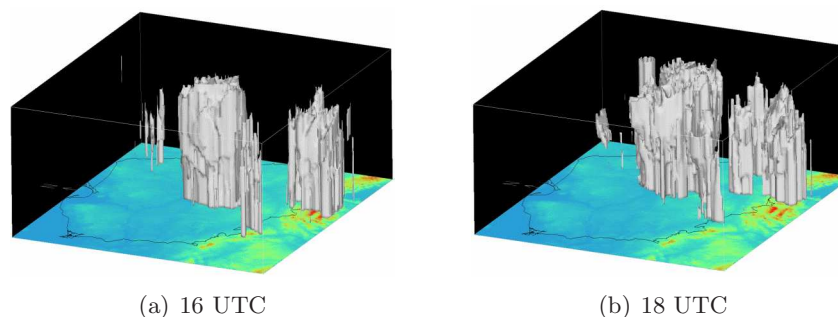


Figure 2: 3D composite model image of radar reflectivity- 20 July 2007

### 3. The detailed, sub-synoptic description of the convective process over southern Poland

To describe the process of convection evolution and to identify different cloudiness forms, characteristic acronyms have been introduced (e.g., HCP = Huge Convective Pattern), and successive numbers have been assigned to them as they appeared in time (see [6]). The abbreviation  $\Rightarrow$  means conversion of one object into another. Each term responds its adequate 3D reflectivity composite, altogether illustrating 4D evolution of the process. Concerning stage [D] (14-16 UTC):

14:00 huge Cb - HCb0607 - consolidates and grows up, slowly propagating eastwards; the CuHCb09ensembleTatry creates a vast cloud complex with a built-in HCb; Cu10 elongates and collocates NE, according to the steering stream.

14:30 - vast HCb0607 is getting anticyclonal rotation (AC), very slowly propagates easterly, enforcing lightning activity trying to get in touch with Cb10; CuHCb09ensembleTatry still active; Cu10 consolidates and very fast (in less than half hour) transforms into huge Cb  $\Rightarrow$  HCb10 and propagates over about 100 km northeasterly. The Brzuchania radar echo top map taken at 14:20 UTC (Fig. 3(a)) is showing these two separated convective cells: HCb0607-A (bigger but lower) and HCb10-B (smaller but higher).

15:00 - HCb0607 transforms into singular huge convective cell HCPCb0607 with two rotating AC tops (cores) huge HCb, and very slowly propagates east, still waiting for huge Cb HCb10 with deduced cyclonic circulation (C); at 14:40Z lightning strokes of two cells merge overtaking their fusion; HCb10 spreads up and enlarges, transforms into huge convective pattern HCPCb10, slows down and catches up HCPCb0607; CuHCb09ensembleTatry creates convective doublet HCPCbdoubletTatry on Polish and Slovakian sides. At 15:30 from these two giant convective patterns, with huge HCb: HCPCb0607 and HCPCb10, after their fusion, there appears the giant supercell Sc060710 (see Fig. 3(b)) with a double core system (one of them is getting transformed into tail; thus fulfilling the supercell definition: mesocyclon core, overshooting and tail); HCPCbdoubletTatry is more vigorous behind the Tatras range on the Slovakian side and weakens on the Polish side  $\Rightarrow$  HCPCbSlovakia.

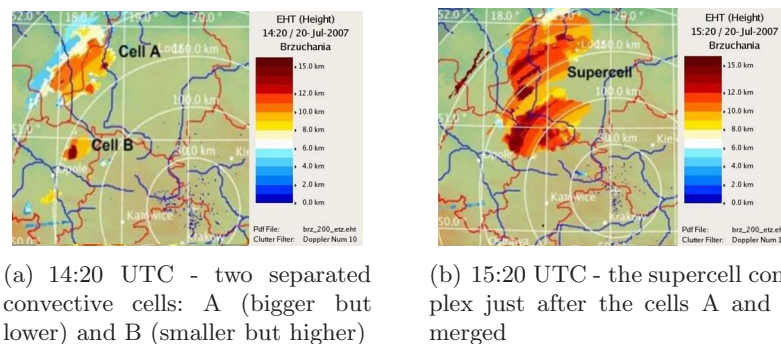


Figure 3: The Brzuchania radar echo top map

16:00 the giant supercell Sc060710, with merged precipitation cores, forms a bow with initial tail stage, on the southern bow periphery, close to tail the tornado is forming at the moment; HCPCbSlovakia; in Jesioniki mountains and Pradziad hill new CPCb11 appear.

17:00 - the giant supercell Sc060710 slowly propagates east, the bow-like precipitation core is now reversed west, the large tail is built-up and directed southwesterly (comment: the west-

ward reversing of the bow and the SW tail direction point to the anticyclonic macrorotation, while the tornados mesocyclon inside supercell should rotate cyclonally; according to the eye-witness, the tornado has extinguished at 16:15); CPCb11 is towering and elongate according to steering stream north-east heading to fuse with tail of Sc060710; HCPCbSlovakia reconsolidates and slightly propagates north.

17:30 - the giant supercell Sc060710 keeps slowly propagating east, the reversed bow like precipitation core regenerates (pulsing); CPCb11 strengthens up north from Pradziad hill still heads towards tail of Sc060710; HCPCbSlovakia weakens.

18:00 - Sc060710 keeps holding slightly weakens; remains strong multi-nuclei precipitation core which transforms from bow into linear form, whereas the tail is keeping its holding. The neighboring systems CPCb11 and HCPCbSlovakia dissipate.

#### 4. How to predict a similar tornado in the future?

*Predictability.* The synoptic analysis of the convective process that has led to a supercell and tornado incident was partially deterministic and partially stochastic. The first macro stage, comprising the 8-day pre-convective period and developing over North Atlantic as a large-scale process, was relatively easy to predict. The second stage, developed over Europe which was providing extraordinary growth of instability and might be limited to one-day forecast was also relatively well predicted by operational NWP model. So, the synoptic background on which the convective process has developed was recognized correctly, at least from synoptic point of view. However, the convective process by itself, which might be confined to convective cloudiness, as it appears and vanishes before aggregation into convective complex, was undoubtedly stochastic. It seems that the game the convective clouds played before 14:40 UTC must remain unpredictable. But since the moment the lightning strokes of huge but slowly convective complex and fast propagating Cb have merged, overtaking their fusion (compare Fig. 4(a)-4(b)), it was clear that we would have a supercell and possibly tornado. Since that moment, parallel processing of radar and lightning data should foresee further supercell development and propagation.

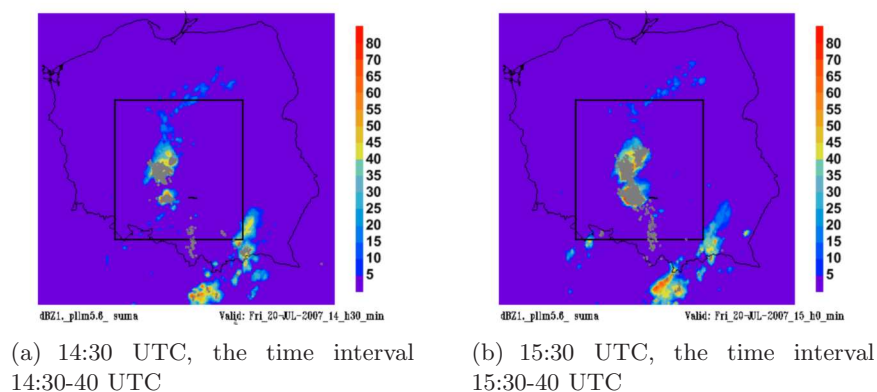


Figure 4: Radar reflectivity map (in dBZ) indicated by colored scale and lightning strokes locations denoted by small grey squares together with tornado location shown by black bar and selected space domain 340x340 km used in our considerations

*The potential of NWP models.* The applied COSMO model computer simulations with different grid resolutions have been used, with the grid step squeezed up to 2.8 km starting from 00 and 12 UTC (Newsletter 9, Fig.11). The typical wind jump and related vortex tube

trace were simulated by the COSMO-Model 2.8 km/50 levels but the problem occurred with convective cloud water structures. The conclusion was that the object that was 30 km wide and 18 km high must not be treated stochastically, and should be reasonably restored by the model.

*The potential of radar wind retrieval.* The significance of the radar reflectivity assimilation in the process of successive absorbing new data and rerunning the dedicated tornado forecasting model is obvious and essential. Typically, the assimilation concept bases on the latent heat release. The assimilation of Doppler wind component is more complicated as the rational way to enhance the models vigor is to include into the data the rotational wind part. This needs application of retrieval technique. Here, a single Doppler retrieval technique has been used to obtain 3D distribution of the tornado-like wind structure showing descending spiral motion with the maximum downward velocity just above the tornado (Newsletter 10).

*The potential of total (IC+CG) lightning rate data.* (after [1], [6]). Many lightning characteristics gathered during supercell event observations, as reviewed and reported recently by Tessendorf, ([9]), have indicated that the IC/CG ratio tends to increase with increasing storm severity and its electrical activity. Thus, this ratio could also be used as an indicator of enhanced severe weather potential. Moreover, (see [3]), basing on his experience with severe and tornado storms in Central Florida (USA), have noticed that sudden increases in the lightning rate, referred to as lightning jumps, have preceded the occurrence of severe weather phenomena by 10 or more minutes. These jumps were typically 30-60 flashes/min<sup>2</sup>, and were easily identified as anomalously large time derivatives of the lightning flash rate. For our case of supercell event (see Fig. 5), one of the local maximum values of time derivative of total lightning rate was of the order 10 strokes/min<sup>2</sup> and occurred about 5 minutes before the visible appearance of tornado.

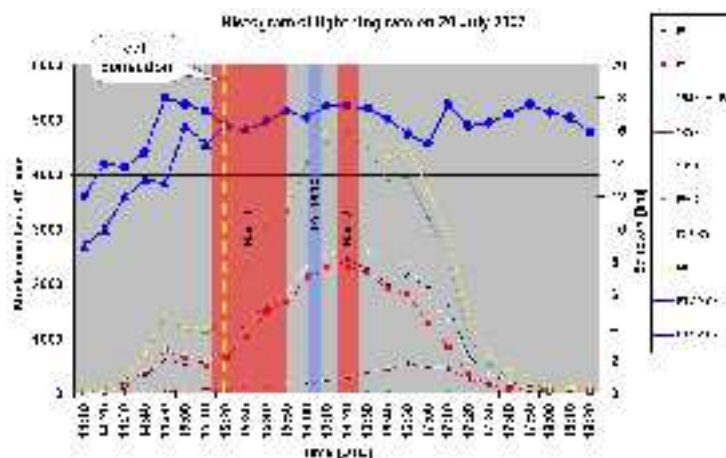


Figure 5: Histogram of lightning frequency for different types of discharges detected by the SAFIR/PERUN network system in the chosen area containing two separated convective cells (see Fig. 3(a)) and the considered supercell complex after cell aggregation (see Fig. 3(b)), i.e., positive and negative return strokes of cloud-to-ground flashes (RS+ and RS), intracloud discharges (IC), and not fully recognized discharges named isolated points (IP). Additionally, the time changes of radar echo top of those cells and supercell are overlapped with the same time interval.

Taking into account the particular stages of dynamic evolution of the considered supercell convective complex and using the space domain that was especially chosen for this purpose, the time variation of frequency of different types of lightning discharges detected by the SAFIR/PERUN network system (see [8], [10]) were examined, i.e., the positive and negative return strokes (RS+ and RS) of cloud-to-ground flashes (CG), intracloud discharges (IC), and other, not fully recognized discharges, isolated points (IP). It was found (see Fig.5) that the first peak of lightning frequency histogram, with a total of 1422 lightning strokes per 10

minute interval and for 4 stroke types detected by the SAFIR/PERUN system, preceded by 25 minutes the onset of first heavy hail gush, by 1 hour and 10 minutes the moment of visible tornado onset, and by 1 and half hour the second episode with heavy hail gush. The next, much more distinct peak of such lightning frequency, with a total of 5065 lightning strokes per 10 minute interval, followed by 65 minutes the onset of first heavy hail gush and by 20 minutes the moment of visible tornado and overlapped with the onset of the second episode with heavy hail gush. The tornado incident was preceded by a meaningful jump of IP and IC counts per 10 minute interval, whereas counts of RS were from 7 to 9 times lower, with nearly the same small number of RS+. As a result, a growing value of the ratio  $IC/RS+RS+$  was obtained - about 6 times greater than that one observed during ordinary thunderstorms in Poland (see [1]).

## 5. Conclusions

Virtual Synoptic Laboratory concept has been adopted to understand the synoptic background on which the convective process has developed. The predictability analysis (phenomenological approach) concerned the potential of particular components of the system, i.e., NWP model output, radar and lightning data. The first macro stage, comprising several days of the pre-convective period and the second one-day forecast stage developing over Europe, which provide necessary growth of instability are hoped to be well predicted by our operational models. However the 3rd stage lasting for a few hours and precede supercell formation has been recognized as difficult to predict. The process of successive absorbing (assimilation) of new radar and lighting data during this period will be essential for tuning the model and extending the successful forecast range. Based on the optimistic facts that: 1) the non-hydrostatic and compressible COSMO model has shown inclination to restore the characteristic typical wind jump and related vortex tube, 2) the assimilation of Doppler rotational wind component provide a quite realistic approximation of the tornados like funnel oscillation, and, 3) that the lightning data occurred to be a good proxy of the visible tornado it seems rational to head for prediction. One of the solutions is a moving nested grid of about 100km wide and 20km high with resolution 0.5km/100m (or less) being accurately positioning every 10 minute accordingly to radar data inflow and stimulating by lighting data assimilation. The alternative would be overlapping, pre-configured nested grids system.

**Acknowledgments:** to Stanislaw Michnowski for inspiring lightning studies, to David Schultz for stimulating comments, to Piotr Baranski (the lighting expert) for close collaboration.

## References

- [1] Baranski, P., P. Bodzak, A. Maciazek, 2002: Some results of the SAFIR, radar and field mill observations for selected thunderstorms near Warsaw. *Abstracts of the 2002 SAFIR Workshop, Budapest*.
- [2] Beblot, G., I. Holda, K. Rorbek, 2007: The tornado in the Czestochowa region on 20 July 2007, *IMGW, Oddzial Krakow, Gornoslaskie Centrum Hydro-Meteorologiczne w Katowicach*, p.18 (in Polish).
- [3] Goodman S.J., D. Buechler, S. Hodanish, D. Sharp, E.R. Williams, R.A. Boldi, A.M. Matlin, M.E. Weber, 1999: Total lightning activity associated with tornadic storms. In: *Proceedings of the 11th Int. Conference on Atmospheric Electricity*, Gunthersville, Alabama, USA, June 7-11, 1999, pp. 515-518.

- [4] Parfiniewicz J., 2008: 20th of July 2007 Explosive Convection over Europe. The COSMO Perspective, 5 Working Group on Verification and Case Studies, *COSMO Newsletter 9* (available at <http://www.cosmo-model.org/content/model/documentation/newsLetters/>), **79 85**
- [5] Parfiniewicz J., Baranski P., Gajda W., 2009: Preliminary Analysis of Dynamic Evolution and Lightning Activity Associated with Supercell Event: Case Story of the Severe Storm with Tornado and Two Heavy Hail Gushes in Poland on 20 July 2007, *PUBLS. INST. GEOPHYS. POL. ACAD. SC.*, D-73 (412), 2009, p.**65 - 88**
- [6] Parfiniewicz J., 2009: Tornado w rejonie Czestochowy - 20 lipca 2007 *Czesc 1: Analiza synoptyczna. Czesc 2: symulacje komputerowe i analiza 3D*. Prz.Geof. LIV, 3-4 s.**147 181**. (in Polish).
- [7] Parfiniewicz J., 2010: Retrieving tornados like wind structure (20.07.2007, Czestochowa, Poland case) using singular radar Doppler velocity , 5 Working Group on Verification and Case Studies, *COSMO Newsletter 10* , p. **70 71**
- [8] SAFIR, 2003: 3000 Software User Manual (Data Analysis Module, DAMen-2.1), Vaisala SA, Europarc de la Sainte Victoire, 13590 Meyreuil, France, July 2003.
- [9] Tessendorf, S.A. 2009: Characteristics of lightning in supercells, Chap. 4, pp. 83-114. In: H.D. Betz, U. Schumann, and P. Laroche (eds.), *Lightning: Principles, Instruments and Applications*, Springer Netherlands, DOI: **10.1007/978-1-4020-9079-0\_4**.
- [10] Vaisala, 2003: SAFIR 30003, User Manual, DS Settings and Control Manual, Release 2.3, Helsinki, Finland, July 2003.